SNOW WATER EQUIVALENT RETRIEVAL FROM SENTINEL-1 INSAR USING A COLLOCATED ACTIVE REFLECTOR AND GNSS REFRACTOMETRY

Paolo Perret[1,2,*], Pedro Espín-López[3], Guido Luzi[3], Martina Lodigiani[2], Lorenzo Silvestri[1], Tommaso Congiu[2], Fabrizio Troilo[2], Francesco Zucca[4], Marco Pasian[1]

[1]*University of Pavia, Department of Electrical, Computer and Biomedical Engineering, Pavia, Italy*
[2]*Fondazione Montagna Sicura, Courmayeur, Italy*
[3]*Centre Tecnològic de Telecomunicacions de Catalunya (CTTC/CERCA), Castelldefels, Spain*
[4]*University of Pavia, Department of Earth and Environmental Sciences, Pavia, Italy*

ABSTRACT: Spaceborne C-band interferometry is sensitive to changes in snow water equivalent (SWE), but it needs a phase reference that is absolute, unambiguous, and restricted to dry snow. We address that requirement with a station that combines a ground-flush C-band active reflector (AR) with a collocated GNSS refractometry antenna, installed at 2166 m in the Aosta Valley, Italian Alps. Both instruments sit at ground level and spend the winter beneath the snowpack.

This paper describes the station, characterises the ground reference it produced over the winter of 2025–2026, and gives a first reading of the radar side. The GNSS antenna returned half-hourly SWE from 19 November to 17 May, 179 days at 82 % availability, with an observed maximum of 292 mm w.e. on 15 March. Against 22 manual snow pits dug beside the station, the 18 that could be paired show a bias of -4.7 mm and a root mean square difference of 14.4 mm, closer during accumulation (12.3 mm) than during ablation (17.9 mm). Compared with a SNOWPACK simulation driven by the local weather station, the GNSS record shows a small but seasonally structured bias, about $+13$ mm while the pack builds and -13 mm while it melts. On one of the two Sentinel-1 tracks that image the site, the interferometric phase of the reflector, converted with the dry-snow relation and referenced to the GNSS at activation, follows the GNSS record to 6.6 mm and the pits to 10.6 mm through the dry season, once the integer cycles hidden by storms are restored, here by hand. The reflector's signal falls to the clutter level at melt onset, marking the end of the dry-snow regime.

The station therefore delivers an autonomous, verifiable SWE reference next to a controlled radar target whose phase can be read as SWE. Automated resolution of the phase ambiguity and the transfer of the reference to the surrounding basin are the subject of ongoing work.

KEYWORDS: snow water equivalent, GNSS refractometry, active radar reflector, InSAR, Sentinel-1, alpine snowpack

1. INTRODUCTION

Snow water equivalent is the quantity that matters for runoff, storage, and water supply, and it is the quantity that mountain observation networks measure least densely. Repeat-pass C-band interferometric synthetic aperture radar (InSAR) offers a route to mapping it, because dry snow delays the radar wave by an amount that depends on the water equivalent of the layer it crosses (Guneriussen et al. 2001; Leinss et al. 2015). Sentinel-1 provides the repeat-pass geometry every six days over most of the Alps.

Turning the interferometric phase into SWE, however, requires a reference, and the reference has to satisfy three conditions at once. It must fix the additive offset that repeat-pass interferometry leaves undetermined, so that a phase difference can be read as an absolute change in SWE. It must resolve the integer ambiguity, since the phase is known only modulo 2π and one cycle at C-band corresponds to roughly 25–30 mm w.e., a value a single storm can exceed between two passes. And it must indicate when the dry-snow assumption fails, because liquid water destroys the relation between phase and water equivalent.

Existing C-band retrievals have relied on in-situ station networks for that reference (Oveisgharan et al. 2024; Zhou et al. 2025). Such networks do not exist in most alpine catchments. The alternative explored here is to concentrate the reference into a single instrumented point: a controlled radar target that stays coherent through the winter, and a collocated sensor that measures the SWE above it directly.

This paper describes the station, assesses the quality of the ground reference it produced during the winter of 2025–2026, and shows what the reflector phase looks like once that reference is applied to it at the station itself.

* *Corresponding author address:*
Paolo Perret, University of Pavia,
Department of Electrical, Computer and Biomedical Engineering,
via Ferrata 5, 27100 Pavia, Italy;
email: paolo.perret01@universitadipavia.it

https://doi.org/10.15788/1790099130

2. SITE AND STATION

2.1. Test site

The station is installed at 2166 m a.s.l. on a gently inclined meadow at Pila, Italian Alps. The site lies inside a ski area, which guarantees winter access for maintenance and manual measurements, and it is flat enough that the snowpack accumulates without the drifting and scouring that complicate the interpretation of a point measurement. An automatic weather station (AWS) and a manual snow-profile site are collocated (Figure 1a,b).

2.2. Sub-snow active reflector

The radar target is an electronic C-band transponder rather than a passive corner reflector. It receives the Sentinel-1 chirp on a microstrip patch array, amplifies it by about 42 dB, and retransmits it towards the satellite through a second array, so that it appears in the imagery as a bright and stable point target at 5.405 GHz with a nominal radar cross section near 40 dBsm. The active design fits into a weatherproof enclosure of about $0.6 \times 0.5 \times 0.2$ m that draws less than 0.6 W and runs from a small battery and solar panel. A passive trihedral of comparable cross section would need a side length of about 1.6 m at C-band and would stand well clear of the ground (Garthwaite 2017).

That difference is what makes the installation possible. The reflector is recessed into a shallow pit with its aperture level with the surrounding ground, so that snow accumulates over it as it does over the undisturbed meadow (Figure 1a). Reflectors mounted on masts or frames disturb the snow around them, and even a thin cover on an inclined face measurably alters the radar cross section (Friedt 2024). The reflector was installed at the end of November 2025 and recovered on 18 May 2026, a deployment covering the full snow season. The site is imaged by two descending Sentinel-1 tracks at a six-day repeat, in VV and VH. On the more oblique track (relative orbit 66, incidence $43°$; hereafter T66) the reflector was detected on every acquisition of the dry-snow period. On the steeper one (relative orbit 139, incidence $34°$) it faded under the deepening dry pack from late January, a behaviour analysed separately, and that track is left out of the reading given below. Point-scale SWE retrieval from the interferometric phase of a reflector of this design was demonstrated at a previous site (Perret et al. 2026).

2.3. GNSS refractometry

A low-cost GNSS antenna is installed a few metres from the reflector, at the same ground level, and likewise spends the winter under the snowpack (Figure 1a). Snow above a buried antenna delays the L-band carrier, and comparing the buried antenna with a reference antenna kept clear of snow yields the water equivalent of the intervening layer (Steiner et al. 2019; Steiner et al. 2022; Koch et al. 2019). The GNSS carrier lies at 1.2–1.6 GHz, roughly a quarter of the Sentinel-1 radar frequency: liquid water, which extinguishes a C-band return, attenuates the L-band carrier far less, so the buried antenna keeps receiving through a melting pack, albeit with reduced accuracy. Two u-blox ANN-MB2 antennas, one on the mast above the maximum snow height and one on the ground, feed two receivers built on the u-blox ZED-X20P module. The short baseline between them is processed with the demo5 fork of RTKLIB (Takasu and Yasuda 2009), and the SWE is read from the bias that the snow induces in the Up component of the baseline (Steiner et al. 2020; Steiner et al. 2022), referred to a verified snow-free epoch. The record is half-hourly. The measurement is autonomous, needs no moving parts and no scale, and estimates SWE without an independent density measurement.

The two instruments are complementary by construction. The reflector provides a phase that is precise but ambiguous and offset. The GNSS antenna provides an absolute SWE that is unambiguous but valid only at one point. Because they sample the same local snowpack a few metres apart, the second can be used to condition the first.

3. REFERENCE OBSERVATIONS

Two references were available at the station. Manual snow pits were dug beside it on 22 dates between 26 November and 22 April, each yielding a depth-integrated SWE from density-cutter profiles (Figure 1b). They span 21–275 mm w.e., and each is assigned an uncertainty of 5 mm plus 10 % of its value, in line with reported cutter accuracies (Proksch et al. 2016). Independently, the SNOWPACK model (Lehning et al. 2002) was run for the collocated profile site, driven by the station AWS. Neither the pits nor the GNSS enter the simulation.

The two references differ in kind. The pits are direct observations, sparse in time and affected by the spatial variability of the snowpack at metre scale. The simulation is continuous, but it inherits

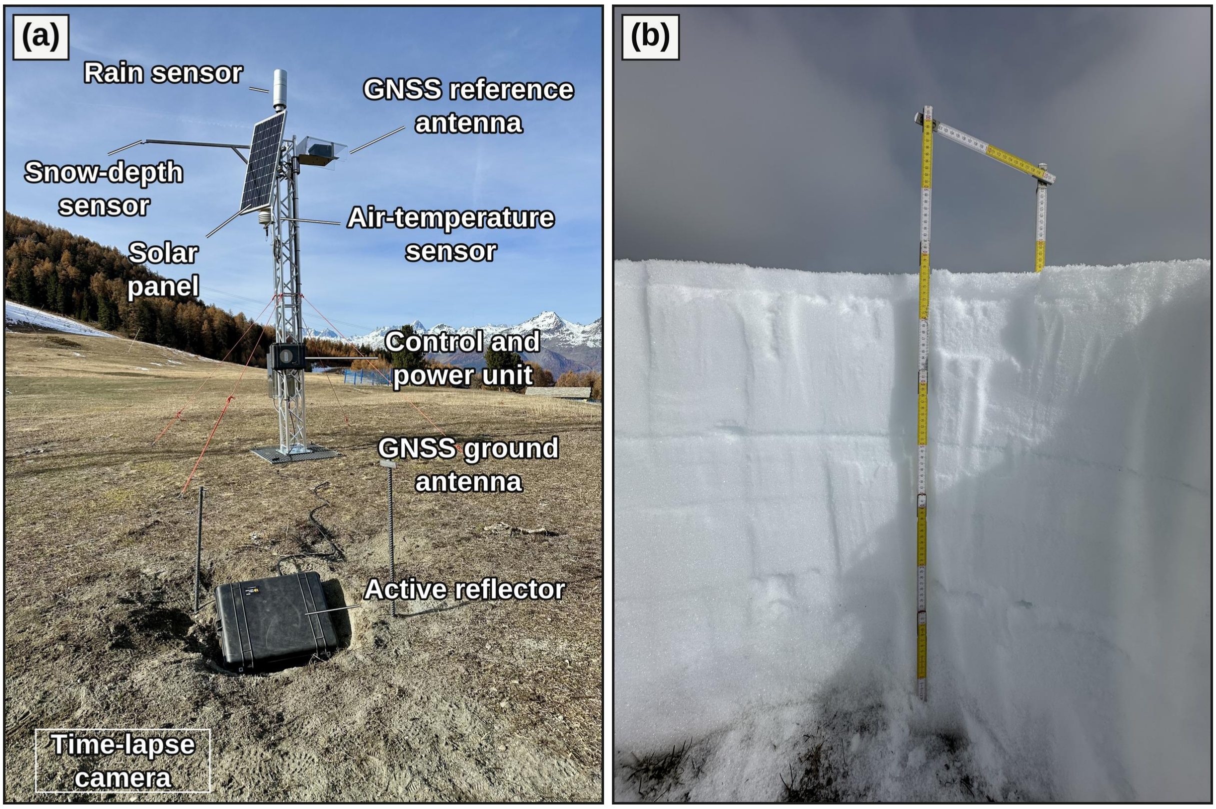

Figure 1: The station at 2166 m. (a) The mast with the GNSS reference antenna and the meteorological sensors, the active reflector flush with the ground, and the GNSS ground antenna (mid-November 2025). (b) One of the 22 manual snow pits dug beside the station (5 March 2026).

the errors of its meteorological forcing, particularly in precipitation, on top of the structural uncertainty of the model itself. Comparing the GNSS record against both is therefore more informative than comparing it against either alone.

4. RESULTS

4.1. Seasonal record

The GNSS station returned half-hourly SWE from 19 November 2025 to 17 May 2026, 179 days over which 82 % of the half-hourly slots carry a valid value (Figure 2a). SWE first exceeded 10 mm w.e. on 24 November and fell below that value on 26 April, giving about five months of snow cover. The largest observed value, 292 mm w.e., was recorded on 15 March. The pack was depleted over the following six weeks.

Continuous operation through the melt season is worth emphasising. Wet snow is the hardest condition to instrument and the one a dry-snow retrieval must exclude. The low carrier frequency lets the GNSS station measure straight through it, supplying precisely what the satellite cannot.

4.2. Comparison with manual measurements

Table 1 compares the GNSS record with the manual pits, using the GNSS value averaged over a window of ± 2 h centred on each measurement. Four of the 22 pits fall inside gaps of the GNSS record and cannot be paired, leaving 18 comparisons. The season is split at the observed maximum on 15 March. The split is a convention rather than a measured turning point, but little rests on it: moved by a week in either direction, it shifts the bias and root mean square difference (RMSD) values of Table 1 by at most about 3 mm w.e.

Over the season the two agree to an RMSD of 14.4 mm, with a bias of -4.7 mm across a range of 21–275 mm w.e. The residuals are not uniformly distributed: during accumulation the agreement is 12.3 mm, and it degrades to 17.9 mm once melt begins, with the sensor reading low relative to the pits. Liquid water changes the propagation the method relies on, so some loss of accuracy in wet snow is expected. Part of the difference is also attributable to the pits themselves, which sample a snowpack that varies at the metre scale, and which cannot be repeated at exactly the same spot. With six ablation pairs, the split statistics describe this

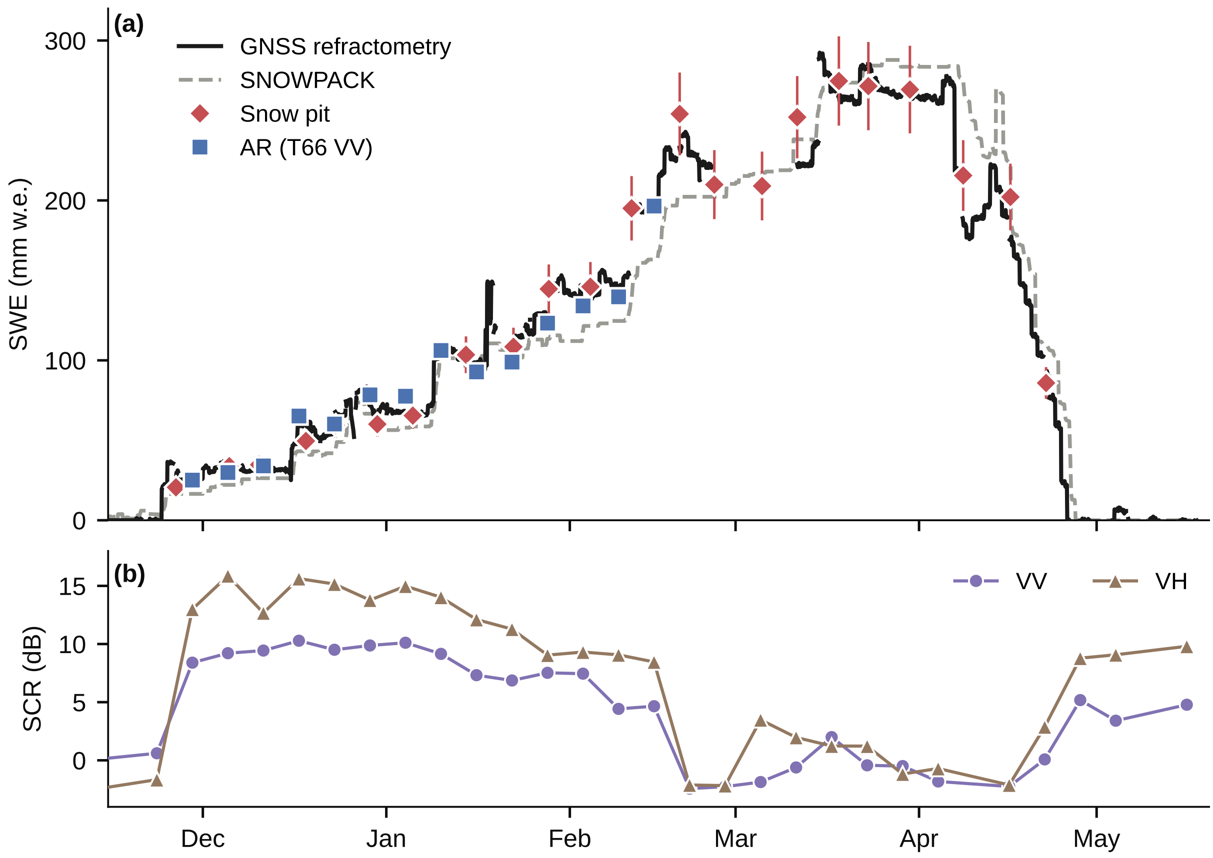

Figure 2: Winter 2025–2026 at the station. (a) SWE from GNSS refractometry, snow pits with their assigned uncertainty, the SNOWPACK simulation, and the reflector phase on T66 converted to SWE (Section 4.4). (b) Signal-to-clutter ratio of the reflector on T66 at each Sentinel-1 acquisition.

sample rather than a general property.

Table 1: GNSS refractometry compared with the manual snow pits and with the SNOWPACK simulation at the station. SNOWPACK sampled on the Sentinel-1 acquisition dates. Bias (GNSS minus reference) and RMSD in mm w.e.

Reference	***Period***	***n***	***Bias***	***RMSD***
Snow pits	Season	18	-4.7	14.4
	Accumulation	12	-2.4	12.3
	Ablation	6	-9.1	17.9
SNOWPACK	Season	46	$+3.7$	21.3
	Accumulation	30	$+12.8$	17.6
	Ablation	16	-13.2	26.8

4.3. Comparison with SNOWPACK

Against the SNOWPACK simulation at the collocated profile site (Table 1), the GNSS record shows a small seasonal bias, $+3.7$ mm, but the average conceals a systematic seasonal structure. While the pack is building, the sensor reads about 13 mm more than the model. While it is melting, about 13 mm less. The model, in other words, both accumulates and depletes the pack more slowly than the GNSS record indicates, and the two effects largely cancel when averaged over the winter.

4.4. SWE from the reflector phase

The purpose of the station is to let the reflector phase be read as SWE, and the winter record allows a first and deliberately simple reading at the station itself. For the more oblique track, T66, the interferometric phase of the reflector was extracted from the coregistered Sentinel-1 images at the activation epoch and at each of the 13 dry-season acquisitions that follow, from 5 December to 15 February, in VV, as a sequence of 13 six-day phase differences. Each difference was converted to a change in SWE with the dry-snow relation of Guneriussen et al. (2001) and Leinss et al. (2015) at the local incidence angle, at which one cycle corresponds to about 25 mm w.e., and the sequence was referenced to the GNSS value at the activation date.

Six of the 13 differences exceed half a cycle, one of them by two whole cycles in the storm of mid-February, and are therefore ambiguous on their own. Their integer cycles were restored by hand against the GNSS record, as in the earlier point-scale experiment (Perret et al. 2026). With those cycles in place, the reflector SWE follows the GNSS to a bias of $+0.3$ mm and an RMSD of 6.6 mm over the nine acquisitions with a valid GNSS value, and the five snow pits dug within a day of an acquisition to -7.0 mm and 10.6 mm (Figure 2a). The two comparisons measure different things: since the GNSS sets the level and decides the cycles, the 6.6 mm describes how consistently the six-day phase increments follow the ground record, while the snow pits provide the independent check.

The amplitude record carries the third piece of information the reference has to provide. The signal-to-clutter ratio of the reflector (Figure 2b) stays between 4 and 10 dB in VV and 8 and 16 dB in VH through the dry season, declining slowly from mid-January, then drops by 7 dB in VV and 11 dB in VH between the acquisitions of 15 and 21 February, when the pack first wets, and stays near zero until the ground reappears in late April. Liquid water attenuates the two-way path through the snow, so the drop marks the end of the dry-snow regime directly at the target, in the same spirit as the backscatter decrease used to map wet snow with Sentinel-1 (Nagler et al. 2016), and it identifies the acquisitions at which the phase reading above must stop.

5. DISCUSSION

Four observations follow from the winter reported here.

First, the combination is practical. A ground-flush active reflector and a ground-level GNSS antenna, the whole station drawing a few watts from a solar panel, operated unattended for a full winter beneath a snowpack of about 1.2 m, and both were recovered intact.

Second, the ground reference is at the right scale for its purpose. An RMSD of 14.4 mm against the snow pits, and 12.3 mm during accumulation, is comparable to half a nominal C-band cycle, which is the scale at which an integer decision has to be made. Whether that is sufficient in every case depends on the combined phase and reference uncertainties and is not evaluated here. The point-scale reading of Section 4.4, in which every one of the six ambiguous differences was decided without hesitation, suggests that it is sufficient at this site.

Third, the seasonal structure of the residuals matters more than their average. Both comparisons degrade in the same direction and at the same time, once the pack begins to melt, and a seasonal mean bias would hide this entirely. For an application that must in any case restrict itself to dry snow, the relevant figure is the accumulation-season agreement, which is the better of the two, and the reflector amplitude tells the retrieval when that season ends.

Fourth, the two halves of the station fit together as intended: the reflector phase, once the GNSS has fixed its level and its cycles, is SWE to within the scatter of the pits. The obvious limitation is that all of this describes one point, one winter, one site, and one of the two tracks. The value of the station is not that it measures SWE at that point, which a snow pillow would also do, but that it does so beside a controlled radar target, which allows the point to be propagated. That propagation, together with the automated resolution of the integer ambiguity and the screening of wet-snow periods across the basin, is the subject of ongoing work.

6. CONCLUSIONS

We have described a compact station that combines a ground-flush C-band active reflector with a collocated GNSS refractometry antenna, and we have characterised the SWE reference it produced during the winter of 2025–2026 in the Italian Alps. The station delivered a half-hourly record over 179 days at 82 % availability, agreeing with the manual snow pits to an RMSD of 14.4 mm with a bias of -4.7 mm, and matching a SNOWPACK simulation to 21.3 mm with a seasonal structure that a single average would conceal. Read against that reference, the reflector phase on one Sentinel-1 track returned the dry-season SWE at the station to within 10.6 mm of the pits, and its amplitude marked the onset of melt. The reference is autonomous, verifiable against independent observations, and continues through the melt season. What SWE retrieval from Sentinel-1 InSAR requires is an absolute level, resolvable cycles, and a flag for wet snow. At Pila, a single low-cost installation provided all three over one full winter.

ACKNOWLEDGEMENTS

This research was supported by Fondazione Montagna Sicura. The authors acknowledge the European Space Agency and the Copernicus programme for providing Sentinel-1 SAR data.

REFERENCES

Friedt, J.-M. (2024). Impact of a Thin Inhomogeneous Snow Layer on a Microwave Corner Reflector RADAR Cross Section: Consequences for Spaceborne Remote Sensing. In: IEEE Transactions on Geoscience and Remote Sensing 62, p. 4301909. https://doi.org/10.1109/TGRS.2024.3423688.

Garthwaite, M. C. (2017). On the Design of Radar Corner Reflectors for Deformation Monitoring in Multi-Frequency InSAR. In: Remote Sensing 9.7, p. 648. https://doi.org/10.3390/rs9070648.

Guneriussen, T., Høgda, K. A., Johnsen, H., and Lauknes, I. (2001). InSAR for Estimation of Changes in Snow Water Equivalent of Dry Snow. In: IEEE Transactions on Geoscience and Remote Sensing 39.10, pp. 2101–2108. https://doi.org/10.1109/36.957273.

Koch, F., Henkel, P., Appel, F., Schmid, L., Bach, H., Lamm, M., Prasch, M., Schweizer, J., and Mauser, W. (2019). Retrieval of Snow Water Equivalent, Liquid Water Content, and Snow Height of Dry and Wet Snow by Combining GPS Signal Attenuation and Time Delay. In: Water Resources Research 55.5, pp. 4465–4487. https://doi.org/10.1029/2018WR024431.

Lehning, M., Bartelt, P., Brown, B., and Fierz, C. (2002). A Physical SNOWPACK Model for the Swiss Avalanche Warning. Part III: Meteorological Forcing, Thin Layer Formation and Evaluation. In: Cold Regions Science and Technology 35.3, pp. 169–184. https://doi.org/10.1016/S0165-232X(02)00072-1.

Leinss, S., Wiesmann, A., Lemmetyinen, J., and Hajnsek, I. (2015). Snow Water Equivalent of Dry Snow Measured by Differential Interferometry. In: IEEE Journal of Selected Topics in Applied Earth Observations and Remote Sensing 8.8, pp. 3773–3790. https://doi.org/10.1109/JSTARS.2015.2432031.

Nagler, T., Rott, H., Ripper, E., Bippus, G., and Hetzenecker, M. (2016). Advancements for Snowmelt Monitoring by Means of Sentinel-1 SAR. In: Remote Sensing 8.4, p. 348. https://doi.org/10.3390/rs8040348.

Oveisgharan, S., Zinke, R., Hoppinen, Z., and Marshall, H. P. (2024). Snow water equivalent retrieval over Idaho – Part 1: Using Sentinel-1 repeat-pass interferometry. In: The Cryosphere 18, pp. 559–574. https://doi.org/10.5194/tc-18-559-2024.

Perret, P., Luzi, G., Espín-López, P., Lodigiani, M., Silvestri, L., Congiu, T., Troilo, F., Zucca, F., and Pasian, M. (2026). "Direct Retrieval of Snow Water Equivalent (SWE) Using the Sentinel-1 Interferometric Phase Response of an Active Reflector". In: The International Archives of the Photogrammetry, Remote Sensing and Spatial Information Sciences. Vol. XLVIII-M-11-2026, pp. 31–37. https://doi.org/10.5194/isprs-archives-XLVIII-M-11-2026-31-2026.

Proksch, M., Rutter, N., Fierz, C., and Schneebeli, M. (2016). Intercomparison of Snow Density Measurements: Bias, Precision, and Vertical Resolution. In: The Cryosphere 10, pp. 371–384. https://doi.org/10.5194/tc-10-371-2016.

Steiner, L., Meindl, M., and Geiger, A. (2019). Characteristics and Limitations of GPS L1 Observations from Submerged Antennas: Theoretical Investigation in Snow, Ice, and Freshwater and Practical Observations Within a Freshwater Layer. In: Journal of Geodesy 93, pp. 267–280. https://doi.org/10.1007/s00190-018-1147-x.

Steiner, L., Meindl, M., Marty, C., and Geiger, A. (2020). Impact of GPS Processing on the Estimation of Snow Water Equivalent Using Refracted GPS Signals. In: IEEE Transactions on Geoscience and Remote Sensing 58.1, pp. 123–135. https://doi.org/10.1109/TGRS.2019.2934016.

Steiner, L., Studemann, G., Grimm, D. E., Marty, C., and Leinss, S. (2022). (Near) Real-Time Snow Water Equivalent Observation Using GNSS Refractometry and RTKLIB. In: Sensors 22.18, p. 6918. https://doi.org/10.3390/s22186918.

Takasu, T. and Yasuda, A. (Nov. 2009). "Development of the low-cost RTK-GPS receiver with an open source program package RTKLIB". In: Proceedings of the International Symposium on GPS/GNSS. Jeju, Korea.

Zhou, J., Lei, Y., Pan, J., Liang, C., Yunjun, Z., Li, W., Xiong, C., Shi, J., and Ma, W. (2025). Snow water equivalent retrieval and analysis over Altay using 12 d repeat-pass Sentinel-1 interferometry. In: The Cryosphere 19.11, pp. 5361–5388. https://doi.org/10.5194/tc-19-5361-2025.